Human Molecular Genetics, 2010, Vol. 19, No. 1 ***181–195***
doi:10.1093/hmg/ddp478
Advance Access published on October 19, 2009

SUMOylation attenuates the aggregation propensity and cellular toxicity of the polyglutamine expanded ataxin-7

Alexandre Janer[1,2‡], Andreas Werner[3†‡], Junko Takahashi-Fujigasaki[4], Aurélie Daret[1,2], Hiroto Fujigasaki[5], Koji Takada[6], Charles Duyckaerts[1,2,7], Alexis Brice[1,2,8], Anne Dejean[3] and Annie Sittler[1,2,*]

[1]INSERM, UMRS 975, CNRS UMR 7225, Paris, France, [2]UPMC/Univ, Paris 6, INSERM UMRS 975, CNRS 7225, Centre de Recherche-Institut du Cerveau et de la Moelle Epinière, Paris, France, [3]Nuclear Organisation and Oncogenesis Unit, INSERM U579, Institut Pasteur, Paris, France, [4]Division of Neuropathology, The Jikei University School of Medicine, Tokyo, Japan, [5]Department of Neurology, Musashino Redcross Hospital, Tokyo, Japan, [6]Department of Biochemistry, The Jikei University School of Medicine, Tokyo, Japan, [7]AP-HP, Assistance Publique Hôpitaux de Paris, Groupe Hospitalier Pitié-Salpêtrière, Laboratoire de neuropathologie, Paris, France and [8]Département de Génétique et Cytogénétique, AP-HP, Assistance Publique Hôpitaux de Paris, Groupe Hospitalier Pitié-Salpêtrière, Paris, France

Received August 7, 2009; Revised October 7, 2009; Accepted October 14, 2009

Post-translational modification by SUMO (small ubiquitin-like modifier) was proposed to modulate the pathogenesis of several neurodegenerative diseases. Spinocerebellar ataxia type 7 (SCA7) is a neurodegenerative disorder, whose pathology is caused by an expansion of a polyglutamine stretch in the protein ataxin-7 (ATXN7). Here, we identified ATXN7 as new target for SUMOylation *in vitro* and *in vivo*. The major SUMO acceptor site was mapped to lysine 257, which is part of an evolutionarily conserved consensus SUMOylation motif. SUMOylation did not influence the subcellular localization of ATXN7 nor its interaction with components of the TFTC/STAGA complex. Expansion of the polyglutamine stretch did not impair the SUMOylation of ATXN7. Furthermore, SUMO1 and SUMO2 colocalized with ATXN7 in a subset of neuronal intranuclear inclusions in the brain of SCA7 patients and SCA7 knock-in mice. In a COS-7 cellular model of SCA7, in addition to diffuse nucleoplasmic staining we identified two populations of nuclear inclusions: homogenous or non-homogenous. Non-homogenous inclusions showed significantly reduced colocalization with SUMO1 and SUMO2, but were highly enriched in Hsp70, 19S proteasome and ubiquitin. Interestingly, they were characterized by increased staining with the apoptotic marker caspase-3 and by disruption of PML nuclear bodies. Importantly, preventing the SUMOylation of expanded ATXN7 by mutating the SUMO site increased both the amount of SDS-insoluble aggregates and of caspase-3 positive non-homogenous inclusions, which act toxic to the cells. Our results demonstrate an influence of SUMOylation on the multistep aggregation process of ATXN7 and implicate a role for ATXN7 SUMOylation in SCA7 pathogenesis.

INTRODUCTION

Spinocerebellar ataxia type 7 (SCA7) is a progressive autosomal dominant neurodegenerative disorder characterized by cerebellar ataxia and visual impairment (1), caused by neuronal loss in the cerebellum and associated structures and degeneration of cone and rod photoreceptors (2). SCA7 belongs to a family of nine neurodegenerative diseases

*To whom correspondence should be addressed at: CRICM-INSERM UMRS 975 – CNRS UMR 7225, Hôpital de la Salpêtrière, 47, Bd de l'Hôpital, Bat. Pharmacie, 75651 Paris Cedex 13, France. Tel: +33 142162205; Email: annie.sittler@upmc.fr
‡A.J. and A.W. contributed equally to this work.
†Present address: Center for Molecular Biology of the University of Heidelberg (ZMBH), 69120 Heidelberg, Germany.

including Huntington's disease, spinobulbar muscular atrophy, dentatorubral pallidoluysian atrophy and spinocerebellar ataxia types 1, 2, 3, 6 and 17, in which a CAG triplet expansion in the DNA results in polyglutamine (polyQ) expansion in the gene product (3). In SCA7, expansion of the polyQ tract from 37 to 460 residues in the ataxin-7 protein (ATXN7) is responsible for the pathology (1). ATXN7 is a component of the TFTC (TBP-free TAF-containing complex) and STAGA (SPT3/TAF9/GCN5 acetyl transferase) chromatin remodeling complexes, implicated in several steps of transcriptional regulation, such as histone acetylation, deubiquitination and deubiquitination and recruitment of the preinitiation complex to promoters (4,5). During pathogenesis, the mutant polyQ expanded protein tends to form nuclear neuronal inclusions. In addition to mutant ATXN7, these inclusions contain other proteins, such as transcription factors, chaperones (6,7), proteasome subunits (6,8) and promyelocytic leukemia (PML) protein (6,9). Interestingly, inclusions also contain ubiquitin, a small protein implicated in post-translational modification (8).

Recently, post-translational modifications have been shown to play a major role during the pathogenesis of polyQ diseases (10). There is increasing evidence implicating modification by the ubiquitin-like protein SUMO (small ubiquitin-like modifier) in numerous neurological diseases including polyQ disorders (10–12). The covalent attachment of SUMO to a lysine residue in the target protein is catalyzed by an enzymatic cascade, consisting of the E1 activating enzyme, the E2 conjugating enzyme (Ubc9) and an E3 ligase. Vertebrates express at least three paralogs of SUMO; however, SUMO2 and 3, which are nearly identical, differ substantially from SUMO1 (13,14). SUMOylation is thought to modify interactions in multi-protein complexes (15). Besides its role as a covalent modifier, SUMO can bind non-covalently to SUMO-interacting motifs, which have been identified in many proteins (16).

Several proteins causing polyQ diseases, such as huntingtin, ataxin-1 or androgen receptor, are reported to be post-translationally modified by SUMO (17–19). Therefore, we examined whether SUMOylation also plays a role in SCA7. We show here that ATXN7 is a new target for SUMOylation *in vitro* and *in vivo*. SUMOylation of lysine 257 in polyQ expanded ATXN7 modulates the aggregation properties and toxicity of the mutant protein, suggesting that this modification plays a role in the pathogenesis of SCA7.

RESULTS

ATXN7 is modified by SUMO at lysine 257 *in vitro* and *in vivo*

To determine whether ATXN7 interacts with components of the SUMOylation machinery, we performed a pulldown experiment using GST-fusions of SUMO1, SUMO2, the E2 enzyme Ubc9 and the E3 ligase PIAS1 together with full length ATXN7-10Q or an N-terminal fragment consisting of amino acids 1–230 produced by *in vitro* transcription/translation using reticulocyte lysate. Figure 1A shows that ATXN7, as well as its N-terminal fragment were able to interact with SUMO1, SUMO2, Ubc9 and PIAS1. No interaction was observed with GST alone.

To look for a potential SUMOylation of ATXN7, we performed an *in vitro* SUMOylation assay using radioactive ^{35}S-labeled ATXN7 from *in vitro* transcription/translation as substrate. After incubation with purified recombinant E1 and E2 enzymes, as well as SUMO and ATP, SUMOylated forms of ATXN7 could be detected by autoradiography (Fig. 1B). In the presence of SUMO1, one band with the typical 20 kDa size shift appeared. In the presence of SUMO2 at least three modified forms were detected. Since SUMO2 is known to form chains, whereas SUMO1 does not, these results suggest that ATXN7 can be SUMOylated on a single lysine residue, either by one SUMO1 molecule or a SUMO2 chain.

To confirm ATXN7 SUMOylation in a human cell line, HeLa cells were transiently transfected with ATXN7 alone or in combination with His-tagged SUMO1. When we co-expressed His-SUMO1, a band of higher molecular weight was observed, which was specifically enriched by a denaturing nickel pulldown, confirming the modification of ATXN7 by SUMO1 at a single site *in vivo* (Fig. 1C).

Since the SUMO E3 ligase PIAS1 bound ATXN7 (Fig. 1A), we investigated whether PIAS proteins could be involved in ATXN7 SUMOylation. All PIAS family members slightly increased the SUMOylation of ATXN7 after cotransfection together with SUMO1 in HeLa cells. Nevertheless, only PIASxβ and surprisingly the catalytic fragment of the unrelated ligase RanBP2 showed a tremendous enhancement of ATXN7 SUMOylation in the *in vitro* assay using recombinant enzymes (see Supplementary Material, Fig. S1), leaving the definite identification of the relevant E3 ligase for further studies.

For analyzing the functional consequences of SUMOylation, we wanted to identify the target lysine in ATXN7 and looked in the sequence for the well-described consensus SUMOylation site Ψ-K-X-E, with Ψ a hydrophobic and X any amino acid. One motif around lysine 257 (V<u>K</u>VE) perfectly matched this site. To determine whether this residue is SUMOylated, we expressed an N-terminal fragment of ATXN7 (amino acids 90–406) as GST fusion in the *E. coli* SUMOylation system previously described (20). In contrast to the original system, we used a SUMO1-T95R variant, which facilitates detection by mass spectrometry, because only the GG dipeptide from SUMO with a mass of 114 Da remains attached to the target peptide after tryptic digestion. The protein was purified using glutathione beads, electrophoresed on an SDS gel and stained by Coomassie Blue. The band corresponding to single SUMOylated ATXN7 was excised from the gel, digested by trypsin and the peptides were analyzed by mass spectrometry. A peptide exactly matching the mass of ^{251}IMTPSVKVEK^{260} bound to GG was detected in the mixture, confirming that lysine 257 was a potential SUMOylation site. Therefore we tested ATXN7 with lysine 257 mutated to arginine in our *in vitro* SUMOylation assay. A lysine 858 to arginine variant was used as a control. Whereas the K858R variant was SUMOylated as efficiently as the wild-type, the K257R mutation almost completely abolished the SUMOylation of ATXN7 with either SUMO1 or SUMO2 (Fig. 1D). Similar results were obtained for the SUMOylation of ATXN7 by SUMO1 in HeLa cells (Fig. 1E). The K257R mutation clearly reduced the amount

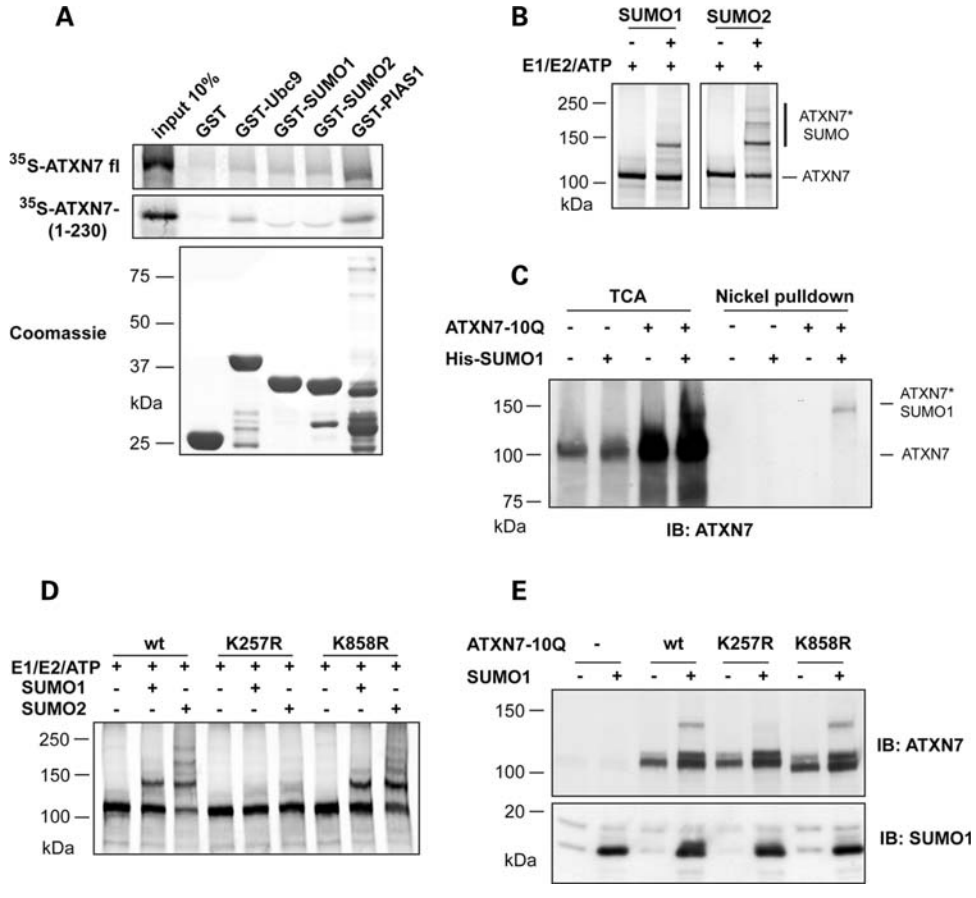

Figure 1. Ataxin-7 is SUMOylated at lysine 257 *in vitro* and *in vivo*. (**A**) Radioactive labeled full length ATXN7-10Q or the N-terminal fragment 1–230 produced by *in vitro* transcription/translation were incubated with purified recombinant SUMO components fused to GST to test for interaction. After GST pulldown the presence of ATXN7 was detected by SDS–PAGE and autoradiography (upper panel). The amount of protein used in the GST pulldown was visualized by loading 25% of the reaction on a Coomassie stained SDS gel (lower panel). (**B**) Radioactive labeled ATXN7-10Q produced by *in vitro* transcription/translation was subjected to an *in vitro* SUMOylation assay in the presence of E1 and E2 enzyme, ATP and either SUMO1 or SUMO2. Reactions were visualized by SDS–PAGE and autoradiography. (**C**) HeLa cells were transfected with ATXN7-10Q alone or in combination with His-tagged SUMO1. Twenty-five percent of the total cell lysate was precipitated with TCA and loaded onto an SDS gel as input control. The remaining lysate was subjected to a nickel pulldown under denaturing conditions. His-SUMO1 modified proteins were separated by SDS–PAGE and detected by western blot using anti-ATXN7 antibodies. (**D**) The ATXN7 variants K257R and K858R were tested for modification in the *in vitro* SUMOylation assay using radioactive labeled ATXN7 from *in vitro* transcription/translation. Reaction products were separated by SDS–PAGE and detected by autoradiography. (**E**) The ATXN7 variants K257R and K858R were transfected into HeLa cells in combination with or without SUMO1. Cell lysates were directly separated by SDS–PAGE and revealed by western blot using anti-ATXN7 antibody. The expression of SUMO1 was detected by anti-SUMO immunoblot.

of SUMOylated ATXN7, whereas the K858R mutation had no effect. This clearly confirms lysine 257 as the major SUMOylation site in ATXN7.

SUMOylation of ATXN7 does not affect its subcellular localization

SUMOylation has been reported to regulate the subcellular localization of several proteins. Therefore, we compared the localization of the wild-type ATXN7-10Q and the SUMOylation deficient variant ATXN7-10Q-K257R in transiently transfected COS-7 cells (Fig. 2A). As previously described, ATXN7-10Q is mainly localized in the nucleus, but is excluded from the DAPI-negative territories corresponding to the nucleolus (Fig. 2Aa, white arrow). The subcellular localization of ATXN7-10Q-K257R was similar to that of wild-type ATXN7-10Q (Fig. 2Ab).

Recently, PML clastosomes in the nucleus have been described to recruit and degrade overexpressed wild-type and polyQ expanded ATXN7 (21). To investigate whether SUMOylation of ATXN7 is involved in this process, we co-expressed wild-type or SUMOylation deficient ATXN7-10Q in COS-7 cells together with isoform IV of the PML protein, which is essential for clastosome formation and function (21). ATXN7-10Q-K257R was recruited by and colocalized with PML IV like wild-type ATXN7-10Q (Fig. 2B). Even if only a small percentage of wild-type ATXN7-10Q is indeed modified by SUMO in cells (see Fig. 1C or E), the fact that the SUMOylation deficient variant K257R was recruited by PML IV demonstrates that SUMOylation of ATXN7 is not a prerequisite for recruitment into clastosomes. Thus, SUMO modification of ATXN7 neither regulates the subcellular localization nor the recruitment to PML clastosomes.

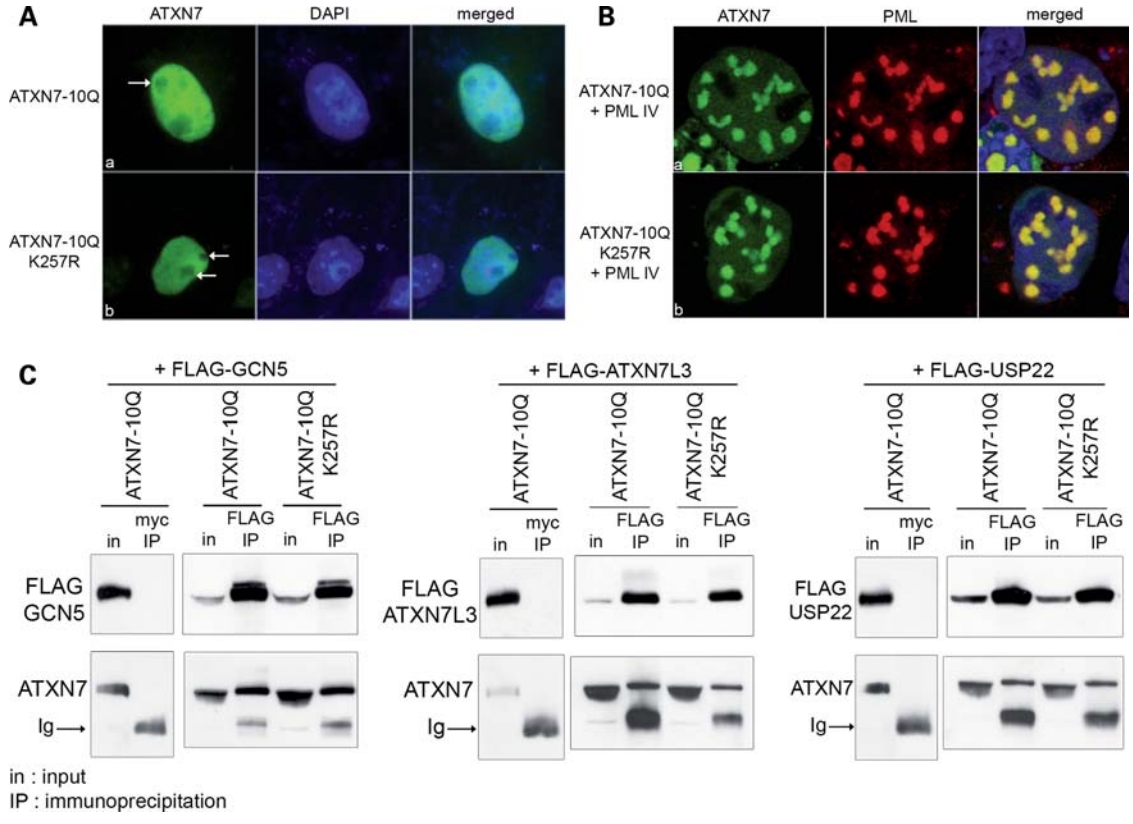

Figure 2. SUMOylation does not influence the subcellular localization of ATXN7 nor its interaction with TFTC/STAGA partners. (**A** and **B**) COS-7 cells were transiently transfected with wild-type HA-ATXN7-10Q or the SUMOylation deficient variant K257R either alone (A) or in combination with PML IV (B). Subcellular localization was analyzed by immunofluorescence after 40 h expression. ATXN7-10Q is localized in the nucleus and excluded from the DAPI-negative territories corresponding to the nucleolus (A, a, white arrow). The subcellular localization of ATXN7-10Q-K257R was similar to that of its wild-type counterpart (A, b). PML isoform IV overexpression leads to the relocalization of ATXN7-10Q inside the PML IV enlarged nuclear bodies, where the two proteins colocalize (B, a). The recruitment within the PML IV nuclear bodies was unaffected by the mutation that renders ATXN7 SUMO deficient (B, b). Anti-PML and anti-HA antibodies were used. (**C**) For co-immunoprecipitation studies, COS-7 cells were transfected with wild-type HA-ATXN7-10Q or the SUMOylation deficient variant K257R in combination with FLAG-tagged GCN5, ATXN7L3 or USP22. After 45 h, the cells were lysed and interactions of ATXN7 with its TFTC partners were tested by co-immunoprecipitation. Partners were immunoprecipitated using an anti-FLAG antibody (top panel). Anti-myc immunoprecipitations were performed as negative controls (top panel). The amount of co-immunoprecipitated ATXN7 was visualized by western blotting against the HA tagged ATXN7 (bottom panel). Similar quantities of ATXN7 were observed to co-precipitate, independently of their SUMOylation status, with FLAG tagged GCN5, ATXN7L3 or USP22. The lower band in the bottom panel corresponds to the heavy chains of immunoglobulins (Ig).

SUMOylation of ATXN7 is not required for its interaction with members of the TFTC/STAGA complex

In TFTC/STAGA chromatin remodeling complexes, ATXN7 interacts with the GCN5 histone acetyltransferase (4) and, together with ATXN7L3 and the USP22 histone deubiquitinase, is part of a deubiquitination module of the complex (5). To determine whether SUMOylation is implicated in the interaction of ATXN7 with TFTC/STAGA complex members, COS-7 cells were cotransfected with the wild-type or SUMOylation-deficient variant of ATXN7-10Q and FLAG-tagged GCN5, ATXN7L3 or USP22. The partners of ATXN7 were immunoprecipitated using an anti-FLAG antibody (Fig. 2C, upper panels) and tested for their interaction with ATXN7 by western blot with an anti-ATXN7 antibody (Fig. 2C, bottom panels). We observed a strong interaction between ATXN7-10Q and GCN5, ATXN7L3 and USP22. However, the levels of co-immunoprecipitated ATXN7-K257R were equivalent to those of wild-type ATXN7-10Q. In conclusion, the interaction of ATXN7 with these TFTC/STAGA components was, therefore, not affected by SUMOylation, at least under overexpression conditions.

SUMO1 and SUMO2 colocalize with polyQ expanded ATXN7 in intranuclear neuronal inclusions

To look for a potential role of SUMOylation in SCA7, we examined the localization of SUMO1 and SUMO2 in the brains of two SCA7 patients (Fig. 3A). Samples of temporal cortex from patient 1, and frontal cortex from patient 2 were chosen because of the relatively high frequency of neuronal inclusions in these areas. We performed single immunolabeling using the anti-ATXN7 (mouse monoclonal 1C1 and rabbit polyclonal 1261), anti-SUMO1 (mouse monoclonal GMP-1 and 3G12, an antibody that we developed, see Supplementary Material, Fig. S2), and anti-SUMO2 (rabbit polyclonal AP1282a) antibodies by conventional DAB staining methods. Numerous ATXN7 positive nuclear inclusions were observed in neuronal cells of the cortex, as previously

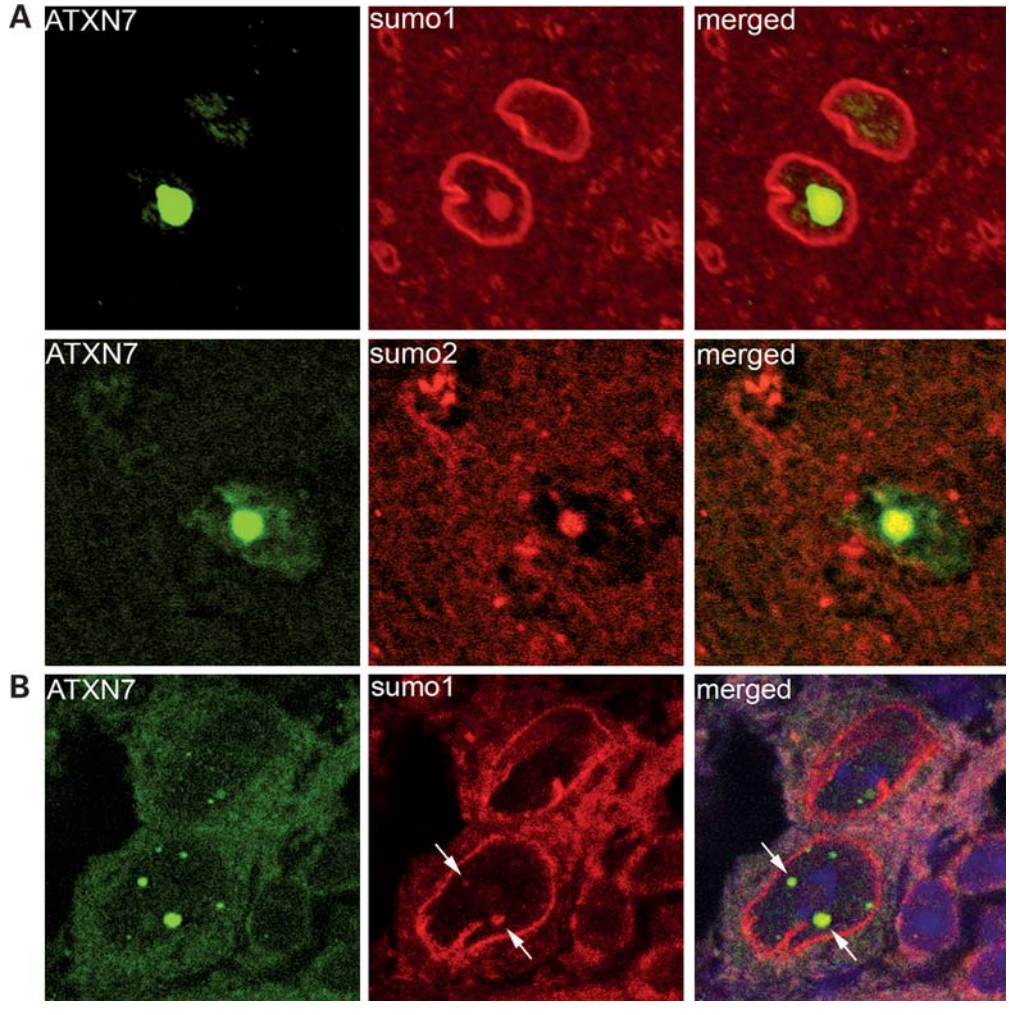

Figure 3. SUMO1 and SUMO2 colocalize with ATXN7 aggregates in brain of SCA7 patients and mice. (**A**) Neurons of the cerebral cortex from SCA7 patients were investigated by double immunostaining, using ATXN7 and SUMO1 or SUMO2 antibodies. SUMO1 preferentially distributed at nuclear membrane and colocalized with ATXN7 in nuclear inclusions. Colocalization of SUMO2 and ATXN7 in nuclear inclusions was also confirmed in the SCA7 patient. Upper panel: double immunolabeling with anti-ATXN7 (1261) and anti-SUMO1 (3G12) antibodies, temporal cortex, patient 1. Lower panel: double immunolabeling with anti-ATXN7 (1C1) and anti-SUMO2 (AP1282a) antibodies, frontal cortex, patient 2. (**B**) Purkinje cells from the cerebellum of a 16-week-old knock-in $Sca7^{266Q/5Q}$ mouse were investigated by immunohistofluorescence using anti-ATXN7 and anti-SUMO1 antibodies. Partial colocalization of SUMO1 with aggregates of polyQ-ATXN7 was observed (white arrows). The same observation was made in different brain regions.

reported (6,8). In addition to known physiological SUMO1 immunoreactivity at the nuclear membrane (22,23), some SUMO1 positive inclusions were found in nuclei. We tested the two independent SUMO1 antibodies, and found that SUMO1 positive inclusions appeared with a low frequency in both of the patients ($<1\%$). Then, we examined the sections double immunolabeled with the anti-ATXN7 (1261) antibody and the SUMO1 (3G12) antibody, and confirmed colocalization of ATXN7 and SUMO1 in nuclear inclusions (Fig. 3A, upper panel). Similarly, the sections immunolabeled by the anti-ATXN7 (1C1) and SUMO2 (AP1282a) antibodies revealed that a small number of the ATXN7 positive inclusions contained SUMO2 epitope (Fig. 3A, lower panel).

Colocalization between SUMO1 and ATXN7 was also seen in the brains of heterozygous SCA7 knock-in mice that express ATXN7 with 266/5 glutamines at endogenous levels and in the proper spatio-temporal pattern of the SCA7 gene (24). The mice, which progressively develop symptoms from 6 weeks of age and die around 15–16 weeks, were analyzed at 16 weeks. SUMO1 colocalized with $\sim$1% of the intranuclear inclusions of mutant ATXN7 in several brain regions (hippocampus, brainstem and cerebellum). Figure 3B shows a representative confocal image where ATXN7 and SUMO1 partially colocalize in Purkinje cells (see white arrows).

Two different forms of inclusions, which differ in their SUMO content, can be distinguished in a cellular SCA7 model

As a cellular model for SCA7, we overexpressed polyQ expanded ATXN7-72Q in COS-7 cells and analyzed the localization patterns of both ATXN7 and SUMO (Fig. 4A). After 2 days of expression, 40% of the cells present a diffuse nuclear staining for expanded ATXN7, which excludes the nucleolus.

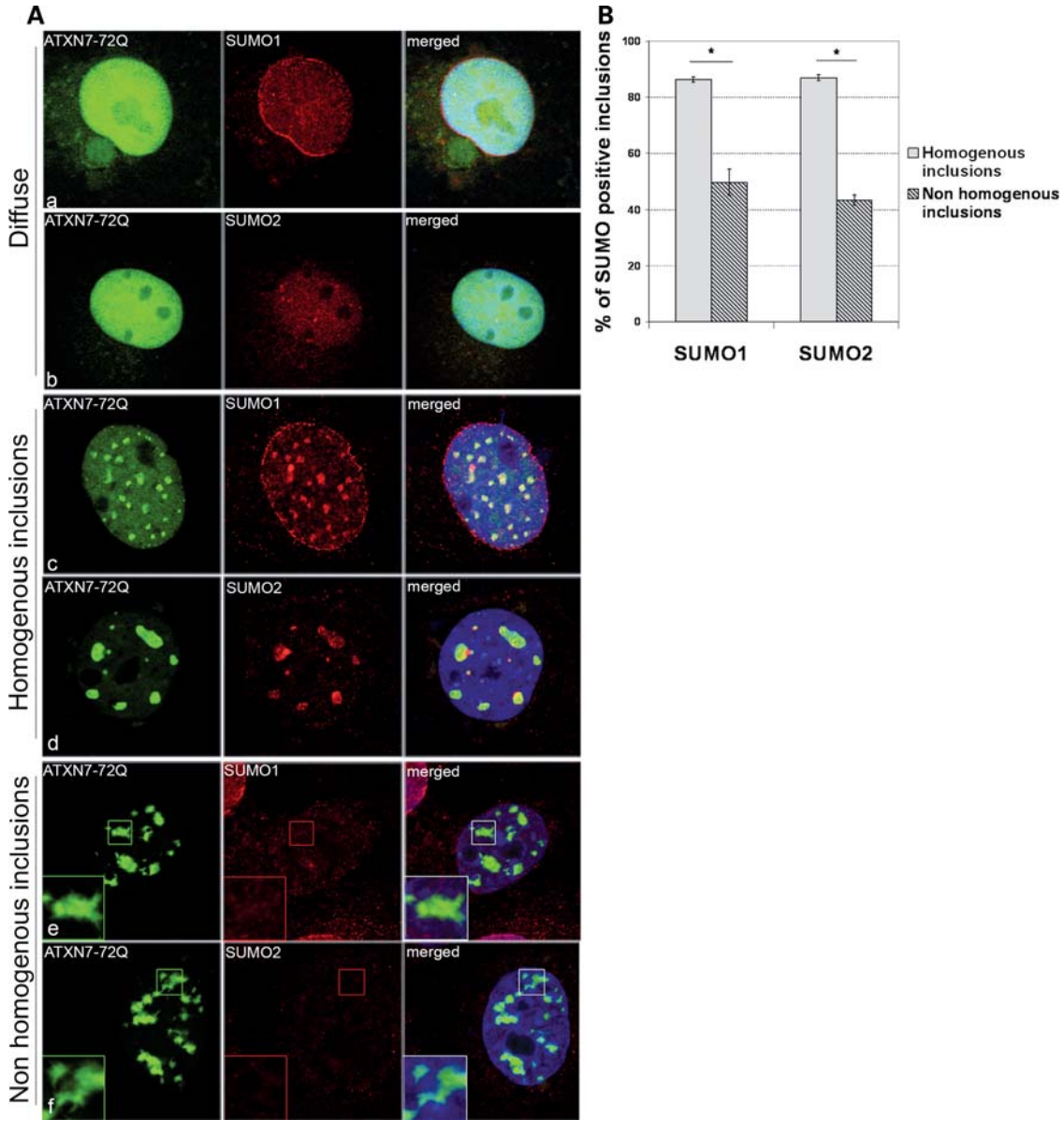

Figure 4. Divers patterns of colocalization between expanded polyQ ATXN7, SUMO1 and SUMO2 in COS-7 cells. (**A**) COS-7 cells were transfected with expanded ATXN7-72Q and immunofluorescence analysis was performed after 48 h. Antibodies used were anti-HA to detect HA-ATXN7 and polyclonal anti-SUMO1 and SUMO2 antibodies. The distribution of expanded polyQ ATXN7 is always nuclear, but three different populations of cells can be distinguished by confocal microscopy: diffuse distribution (40% of the cells, a and b), homogenous inclusions, that are compact, often round (50% of the cells, c and d) and non-homogenous inclusions, with rough edges and structures that stick out of the aggregate (10% of the cells, e and f, see magnification). The SUMOylation pattern varies accordingly: homogenous inclusions colocalize very well with both SUMO1 (86%) (c) and SUMO2 (87%) (d), whereas the non-homogenous inclusions show reduced colocalization with SUMO1 (49%) (e) and SUMO2 (43%) (f). (**B**) Quantification of the percentage of SUMO1 and SUMO2 colocalization with the two types of nuclear inclusions. Three hundred cells containing either homogenous or non-homogenous inclusions were scored for their content in SUMO1 and SUMO2 ($n = 4$). Results are presented as means $\pm$ SEM. Statistical analysis was performed using the Student's *t*-test. Asterisks indicate statistically significant difference ($P < 0.05$).

In these cells, SUMO1 staining was seen at the nuclear membrane and in small dot-like structures, likewise the SUMO2 staining in dot-like structures (Fig. 4Aa and b). These dots most probably correspond to the PML nuclear bodies, as PML is well known to be SUMOylated. In addition to cells with diffuse nuclear ATXN7 staining, we could distinguish two differently shaped forms of nuclear inclusions using confocal microscopy. Fifty percent of the expanded ATXN7 expressing cells formed homogenous inclusions, which are mostly round and compact structures that highly colocalize with SUMO1 (86%) and SUMO2 (87%) (Fig. 4Ac and d). Moreover, 10% of the cells presented large non-homogenous inclusions characterized by a rough 'star-like' edge with radiating fibers or structures that stick out of the inclusions (Fig. 4Ae and f, see magnification). Interestingly, less of these non-homogenous structures colocalized with SUMO1

and SUMO2 (49 and 43%, respectively) compared with the homogenous inclusions. Figure 4B illustrates the quantification of four independent immunofluorescence experiments, in which 300 cells have been counted, and demonstrates the difference of SUMO composition of these two forms of inclusions.

Interestingly, in this cellular model, neither the E2 SUMO-conjugating enzyme Ubc9 nor the different PIAS E3 ligases colocalized with inclusions (data not shown), supposing that they are not trapped in these structures. Assuming that the observed colocalization is at least partially due to covalent attachment of SUMO to ATXN7, these results suggest that the SUMOylation status of the polyQ expanded ATXN7 potentially influences its aggregation properties and that the non-SUMOylated expanded ATXN7 is more prone to form large non-homogenous structures.

Non-homogenous inclusions are enriched in components of the ubiquitin-proteasome system and activated caspase-3 and are associated with the disruption of PML bodies

To better characterize the two kinds of inclusions, we quantified their colocalization with components of the protein folding and degradation machinery. As already described (6–8), homogenous inclusions contained the chaperone Hsp70, the 19S proteasome regulatory subunit as well as ubiquitin that co-localized to 27, 36 and 42% of the inclusions, respectively (Fig. 5A). The colocalization was roughly doubled in cells containing non-homogenous inclusions to 79% for Hsp70, 80% for 19S proteasome and 92% for ubiquitin (Fig. 5A and Ba–c).

To compare the cellular toxicity of the inclusions, we used labeling with an antibody against activated caspase-3, which is a common apoptotic marker. Whereas only 4% of the cells with homogenous inclusions were stained, this number dramatically increased to 55% for cells containing non-homogenous inclusions (Fig. 5A and Bd).

To better understand the differences in toxicity of the two kinds of inclusions, we investigated the link to PML nuclear body (NB) structure and clastosome formation, as we previously showed their importance in the degradation of mutant ATXN7 (21). PML staining in untransfected cells is distributed in small dots typical of PML nuclear bodies in 90% of the cells (Fig. 6Aa). We looked at the distribution of PML for each of the three ATXN7 patterns observed after expressing ATXN7-72Q (Fig. 6A and B). Three hundred cells from each pattern were classified according to the observed PML distribution. In both, homogenous and non-homogenous inclusions, the regular small PML bodies were observed in 29 and 26% of the cells, respectively (Fig. 6B). Interestingly, enlarged PML bodies, reminiscent of clastosomes, were detected in ~28% of the cells with a diffuse nucleoplasmic ATXN7 pattern and in 64% of the cells containing homogenous inclusions (Fig. 6Ab and c and B). In the homogenous inclusion pattern, not every inclusion was next to a clastosome, but usually we detected one or two clastosomes, colocalized or juxtaposed to an inclusion (Fig. 6Ac). Interestingly, at the position of the clastosome, no or very little ATXN7 staining could be detected, suggesting that ATXN7 had been degraded. Importantly, in the non-homogenous ATXN7 inclusions, very few cells with clastosomes were seen. Instead, PML protein was found, in 65% of the cells, either diffuse in the nucleus or faintly colocalized with inclusions with the rough 'star-like' radiating structures of ATXN7 (Fig. 6Ad and B).

Taken together these results suggest that cells formed clastosomes as a trial to degrade the mutant ATXN7 accumulated in the nucleus. The disruption of PML clastosome is an indication that these cells may have lost the ability to degrade mutant ATXN7, are overloaded and apoptotic, as attested by their high content of activated caspase-3.

SUMOylation decreases the aggregation propensity and cellular toxicity of expanded polyQ ATXN7

To investigate the influence of the SUMO modification on the ATXN7 aggregation behavior, we first determined whether a polyQ expansion affects the SUMOylation of ATXN7. We expressed ATXN7-10Q and ATXN7-72Q or their corresponding K257R variants together with SUMO1 in HeLa cells and observed no differences in the SUMOylation pattern (Fig. 7A), demonstrating that the polyQ expansion does not interfere with SUMOylation at lysine 257.

Since SUMOylation was shown to positively or negatively modulate the formation of inclusions in other polyQ disorders (19,25,26), we directly compared the aggregation properties of the polyQ expanded ATXN7 to a SUMOylation deficient variant in COS-7 cells. A quantification of four independent immunofluorescence studies demonstrated that the SUMOylation deficient ATXN7-72Q-K257R forms twice as much non-homogenous inclusions as the wild-type protein (21 and 10%, respectively) (Fig. 7B). Furthermore, we performed biochemical studies evaluating the amounts of the soluble monomer of polyQ expanded ATXN7 or SDS-insoluble aggregates in cell lysates by western blot or filter retardation assay, respectively (Fig. 7C). As expected, ATXN7-72Q was SUMOylated in the lysates used (Fig. 7C, upper panel, arrowhead), whereas the K257R variant was not (Fig. 7C, upper panel). The filter retardation assay revealed that ATXN7-72Q-K257R forms more SDS-insoluble aggregates than the wild-type protein (Fig. 7C, bottom panel). The quantification of four independent filter retardation assay experiments (Fig. 7D) gave rela-

Figure 5. The non-homogenous inclusions of polyQ expanded ATXN7 are enriched in components of the ubiquitin–proteasome system and are toxic for cells. (**A**) Quantification of the colocalization of homogenous and non-homogenous ATXN7-72Q inclusions with the chaperone Hsp70, the 19S proteasome regulatory subunit, ubiquitin and activated caspase-3. COS-7 cells were transfected with expanded ATXN7-72Q and analyzed by immunofluorescence after 48 h. Three hundred cells from each inclusion pattern were counted and scored for colocalization with ubiquitin–proteasome system components and activated casapase-3 ($n = 4$). Results are presented as mean percentages ± SEM. Statistical analysis was performed using the Student's *t*-test. Asterisks indicate statistically significant difference ($P < 0.05$). The colocalization in non-homogenous inclusions was tremendously increased for Hsp70 (79 versus 27%), 19S proteasome (80 versus 36%), ubiquitin (92 versus 42%) and activated caspase-3 (50 versus 4%) compared with homogenous inclusions. (**B**) Immunofluorescence study illustrating the strong colocalization of the non-homogenous inclusions of ATXN7-72Q with Hsp70 (a), 19S proteasome (b), ubiquitin (c) and activated caspase-3 (d).

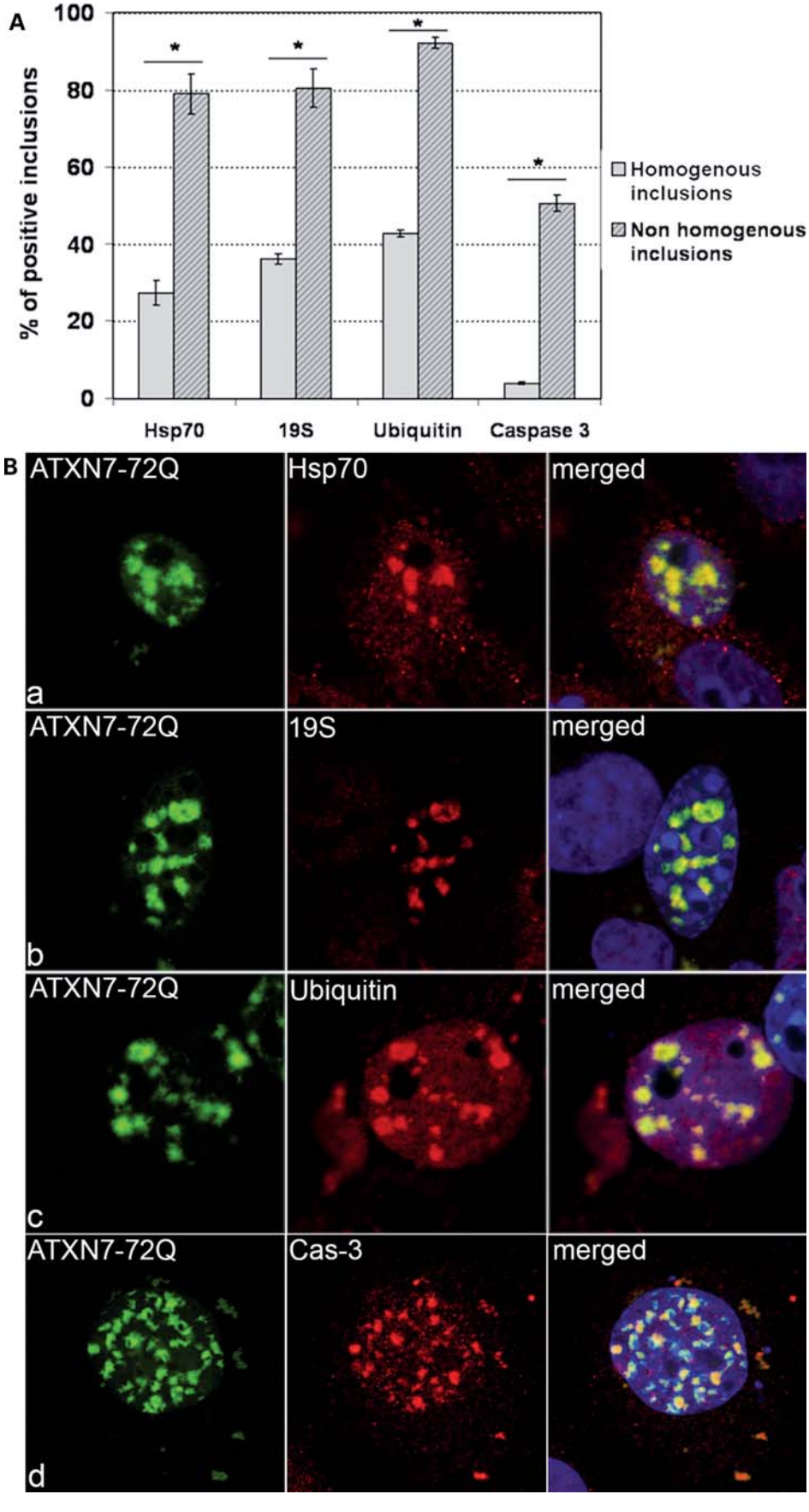

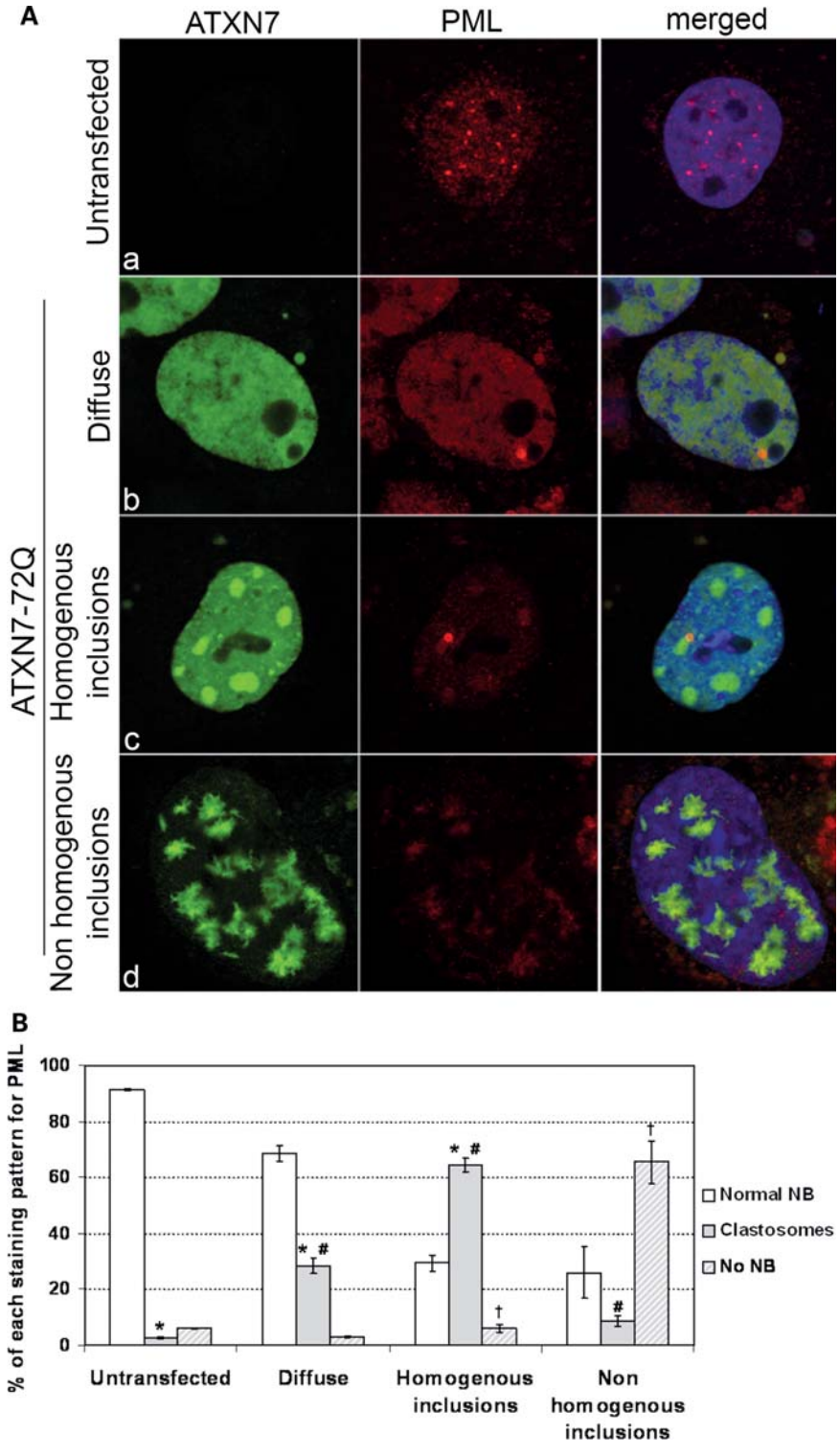

Figure 6. The non-homogenous inclusions of polyQ expanded ATXN7 disrupt the PML nuclear bodies. (**A**) COS-7 cells were transfected with expanded ATXN7-72Q. After 48 h, the distribution of the PML protein was visualized by immunofluorescence. In untransfected cells, the typical dot-like pattern of PML protein corresponding to PML nuclear bodies (NB) was observed (a). In cells expressing ATXN7-72Q, the various patterns of ATXN7 were associated to distinct distributions of PML protein. Thirty percent of cells with a diffuse staining for ATXN7-72Q present a large round and sometimes ring-like PML structure reminiscent of clastosomes (b), which is more often observed in cells with homogenous inclusions (64%) (c). In cells containing non-homogenous inclusions, the PML clastosome structure is disrupted (65%) and PML protein is found diffuse in the nucleus or faintly colocalizes with inclusions (d). (**B**) Quantification of the different PML staining patterns within untransfected or ATXN7-72Q expressing cells. Three hundred cells representing either a diffuse staining, homogenous inclusions or non-homogenous inclusions were scored for the different PML staining pattern ($n = 4$). Results are presented as means $\pm$ SEM. Statistical analysis was performed using the Student's *t*-test. Asterisk, hash, and dagger indicate statistically significant difference ($P < 0.05$). The majority of untransfected cells present a typical PML nuclear bodies structure (91%), whereas only 2% have a clastosome-like staining for PML protein. Twenty-eight percent of the cells with a diffuse ATXN7-72Q staining present a clastosome-like PML pattern. This value reaches 64% in cells with homogenous inclusions. Only 8% of the cells with non-homogenous inclusions present a clastosome-like staining for PML and 65% present a diffuse nuclear PML staining and disrupted PML nuclear bodies.

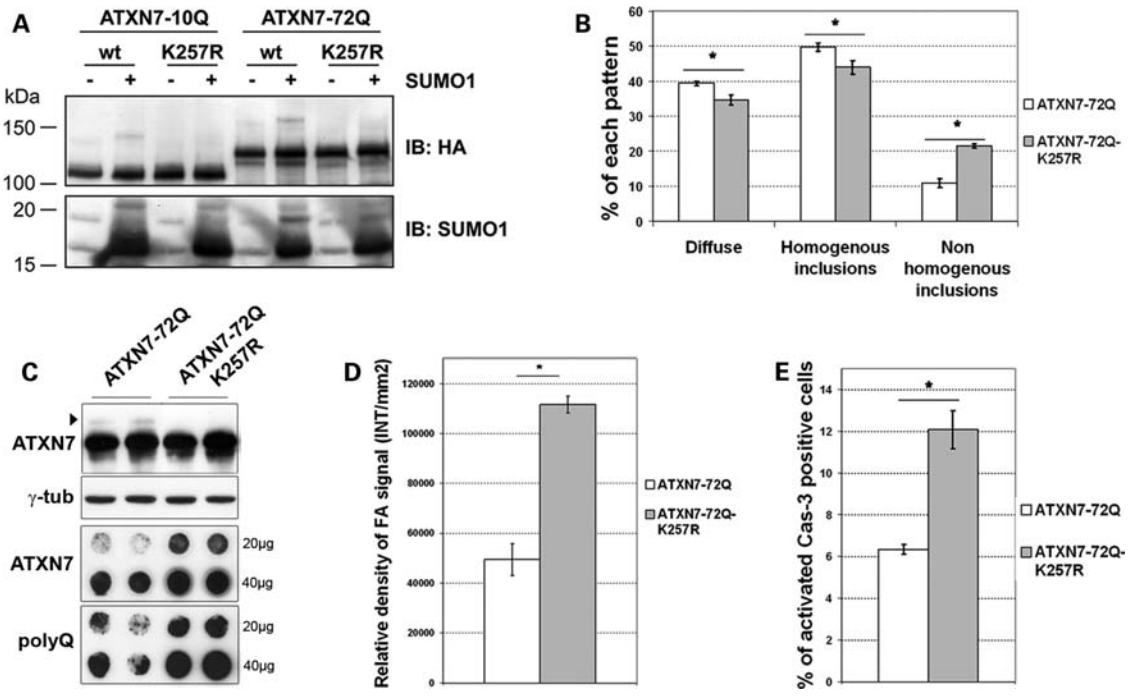

Figure 7. SUMOylation decreases the aggregation propensity and cellular toxicity of expanded polyQ ATXN7. (**A**) HA-ATXN7-10Q or HA-ATXN7-72Q, either wild-type or K257R variant, were transfected into HeLa cells in combination with or without SUMO1 to elucidate the consequences of the polyQ expansion on ATXN7 SUMOylation ability. Cell lysates were directly separated by SDS–PAGE and revealed by western blot using anti-HA antibody. The expression of SUMO1 was detected by anti-SUMO1 immunoblot. The polyQ expanded ATXN7 is SUMOylated as efficiently as the wild-type protein. (**B**) ATXN7-72Q, either wild-type or its SUMOylation deficient K257R variant, was transfected into COS-7 cells and the three distribution patterns of ATXN7 shown in Figure 4 were quantified on 300 cells using immunofluorescence after 2 days expression ($n = 4$). Results are presented as mean percentages $\pm$ SEM. Statistical analysis was performed using the Student's *t*-test. Asterisks indicate statistically significant difference ($P < 0.05$). The SUMOylation-deficient polyQ expanded ATXN7-K257R forms more non-homogenous inclusions compared with the wild-type protein (21 and 10%, respectively). (**C**) The lysates of COS-7 cells with polyQ expanded ATXN7-72Q or its SUMOylation deficient variant (ATXN7-72Q- K257R) were analyzed by western blot after 3 days expression for the level of the soluble monomer (upper panel) and by filter assay for the amount of SDS-insoluble aggregates (lower panel). Tubulin was used as control for equal loading of the western blot (γ-tub). Twenty or 40 μg of total cellular protein were used for the filter assay and anti-ATXN7 (monoclonal 1C1) or an antibody recognizing expanded polyQ stretch (1C2) was used to reveal the membrane. Duplicate results from two independent transfections are presented for western blot and filter assay. As expected, ATXN7-72Q was SUMOylated (upper panel, arrowhead), whereas the K257R variant was not. The filter retardation assay demonstrated that the SUMOylation deficient ATXN7-72Q-K257R forms more SDS-insoluble aggregates than the wild-type protein. (**D**) Quantification of the filter assays (FA) from four independent experiments. Relative densities of each signal were determined and results are presented as mean intensities per $mm^2 \pm$ SEM for ATXN7-72Q and its K257 variant. Aggregation is 2.3$\times$ more pronounced in the SUMO deficient K257R than in the WT 72Q. Statistical analysis was performed using the Student's *t*-test. Asterisk indicates statistically significant difference ($P < 0.05$). (**E**) Quantification of the percentage of activated caspase-3 positive cells expressing ATXN7-72Q or its K257R variant. After 2 days expression, COS-7 cells were stained for ATXN7 and activated caspase-3. Three hundred cells expressing ATXN7 or its K257R variant were counted ($n = 4$). Results are presented as mean percentages $\pm$ SEM. Statistical analysis was performed using the Student's *t*-test. Asterisks indicate statistically significant difference ($P < 0.05$). The SUMOylation deficient polyQ ATXN7 is twice more toxic for cells as the wild-type protein (12 and 6% of colocalization with activated caspase-3, respectively).

tive densities of 111 000 and 49 000 INT/mm^2 for the SUMOylation deficient variant and its wild-type counterpart, respectively. Our results point to a direct effect of SUMOylation on the propensity of expanded polyQ ATXN7 to aggregate. To link these results to the pathogenesis, we finally analyzed the influence of SUMO modification on the cellular toxicity induced by polyQ expanded ATXN7. COS-7 cells expressing either the expanded ATXN7-72Q or its SUMOylation deficient variant were immunolabeled for ATXN7 and activated caspase-3, in order to identify cells in an apoptotic phase. The quantification of four independent immunofluorescence studies indeed demonstrated that ATXN7-72Q-K257R is approximately twice as toxic for cells as the wild-type (12% of activated caspase-3 positive cells compared with 6%) (Fig. 7E). In summary, preventing SUMOylation of expanded ATXN7 in COS-7 cells leads to higher amounts of non-homogenous aggregates, which correlates with a greater amount of SDS-insoluble aggregates and a higher frequency of activated caspase-3 expression.

DISCUSSION

ATXN7, a new SUMO target

In this study, we described ATXN7 as a new target for post-translational modification by SUMO, defining lysine 257 as the major acceptor site. The potential importance of SUMO modification at lysine 257 is highlighted by the complete conservation of the SUMO acceptor site throughout the species from human to zebrafish (see Supplementary Material, Fig. S3). Furthermore, the ATXN7 yeast homologue sgf73 has been identified in two independent screens for new SUMO targets (27,28) suggesting that the yet unknown physiological function of ATXN7 SUMOylation is even conserved

in yeast. Regarding the role of ATXN7 SUMOylation, it is quite striking that after mutating the acceptor lysine, the SUMOylation is nearly completely abolished even under overexpression conditions for SUMO. For many proteins, the SUMOylation machinery evades the mutation of the major acceptor site by attacking adjacent lysine residues (29). The clear restriction to lysine 257 in ATXN7 points to a well-defined role for the modification. As several SUMO E3 ligases enhanced the SUMOylation of ATXN7 *in vivo* or *in vitro*, the identification of the physiologically relevant ligase will be a challenge for future investigations.

Within the TFTC/STAGA chromatin remodeling complex ATXN7 directly interacts with the histone acetyltransferase GCN5 (4) and belongs to a deubiquitination module with ATXN7L3 and USP22 (5). Interestingly, three members of the TFTC/STAGA complex, GCN5, Ada3 and Spt7, are SUMOylated in yeast and SUMOylation of GCN5 reduced the TFTC/STAGA dependent transcription (30). Because SUMOylation is known to modify protein–protein interactions, we compared ATXN7 and its SUMOylation deficient variant for their ability to bind GCN5, ATXN7L3 or USP22. We found a strong, but SUMOylation-independent interaction with all three TFTC/STAGA components, suggesting that SUMOylation of ATXN7 is not involved in regulating the interaction to these proteins.

Besides the modulation of protein interactions, modification by SUMO is described as targeting signal to subcellular structures in or outside the nucleus (22,31–33). However, when we compared ATXN7 and its SUMOylation deficient variant, we could not detect any difference in the subcellular localization of ATXN7 or its recruitment by PML clastosomes, keeping in mind that due to the small amount of SUMOylated ATXN7 present in cells very temporary or local changes can easily be overlooked under overexpression conditions.

Implication of ATXN7 SUMOylation in the SCA7 pathogenesis

Polyglutamine disorders are characterized pathologically by the accumulation of protein aggregates within neurons. This multistep process implicates several intermediates, which differ in structure, solubility and toxicity (34–36). Whether the microscopically visible inclusions play a causal role in disease pathogenesis or protect neurons from the affects of toxic proteins remains unclear (37,38). Therefore, as a central pathological event in polyQ disorders, aggregation needs to be better understood, particularly from a therapeutic point of view.

Several recent reports describe an implication of the SUMO pathway in the pathogenesis of chronic neurodegenerative diseases (10–12,39). Many of the key proteins in these disorders are SUMO targets, among them the three polyQ containing proteins ataxin-1 (18), huntingtin (19) and androgen receptor (17). The colocalization of the neuronal intranuclear inclusions with SUMO in several polyQ disorders raised the question for a role of the SUMO pathway in the pathogenesis (26,40). However, a direct implication of SUMOylation of the disease causing protein has been demonstrated for ataxin-1, huntingtin and androgen receptor (18,19,25), while indirect consequences through global impairment of the SUMO pathway were also suggested in DRPLA and SBMA (26,41). Thus, how SUMOylation could influence the pathogenesis of polyQ disorders is not completely understood and needs further investigations.

Here we show that, as described for several other neurodegenerative disorders, SUMO1 and SUMO2 partially colocalize with ATXN7 inclusions in the brain of SCA7 patients and SCA7 mice, suggesting an implication in physiopathology. In our cellular model, we could distinguish between two different forms of ATXN7 inclusions. Of these two, the large non-homogenous inclusions, those showed significant less colocalization with SUMO, are often stained for Hsp70, 19S proteasome, ubiquitin and activated caspase-3 and thus seem to be more toxic for cells. Accordingly, when the SUMOylation deficient ATXN7-72Q-K257R is expressed, we observed an increased percentage of cells with non-homogenous inclusions. This correlated with a larger quantity of SDS-insoluble aggregates as well as with the doubling in the number of apoptotic cells. Altogether these results suggest that the SUMO deficient polyglutamine expanded ATXN7 could be more prone to aggregate and form the toxic non-homogenous inclusions.

In the brain of patients with SCA7 and other polyQ disorders, in neurons, the PML protein forms large round or ring-like PML nuclear bodies that colocalize with or juxtapose to inclusions (6,9). We demonstrated previously, in a cellular model of SCA7, that these particular PML nuclear bodies called clastosomes, played a role in the degradation of expanded polyQ ATXN7 (21). Here we observed that the formation of the non-homogenous inclusions correlates with the disruption of the PML clastosomes. In these conditions, we could imagine that the PML clastosomes failed to degrade the strongly aggregated mutant ATXN7, became overloaded, which finally lead to their disruption. It is still unclear, if the cells at one point switch to a new phenotype with non-homogenous inclusions, characterized by an enrichment in Hsp70 and ubiquitin components and loss of SUMO colocalization as well as clastosomes, or if the two kinds of inclusions are indicative of two different aggregation pathways. Our observations are supported by studies in SCA7 patient's brain, where large PML nuclear bodies preferentially colocalize with small inclusions but disappear in neurons with large aggregates (6,9). Altogether, our results demonstrate that, by modulating the aggregation process of expanded polyQ ATXN7, SUMOylation of lysine 257 plays a key role in pathogenesis.

These data add to similar observations in other polyQ disorders, in which the SUMO modification of the disease causing proteins influences their aggregation and toxicity. Thus, in Huntington disease, the SUMOylation of a pathogenic huntingtin fragment in cultured cells reduces the number of visible microscopic inclusions and a heterozygous mutation in the SUMO homolog smt3 in Huntington disease drosophila reduces neurodegeneration (19). SUMOylation of the polyQ expanded androgen receptor decreases the amount of both the SDS-insoluble aggregates but also the soluble oligomers (25). A very recent study proposed that SUMOylation may explain the intriguing and not yet understood cell death selectivity observed in polyQ disorders. Briefly, the authors described that Rhes, a striatal specific protein,

increases SUMOylation and toxicity of pathogenic huntingtin (42). In contrast to ataxin-1 (18), polyQ expansion of ATXN7 did not influence its SUMOylation, meaning that the pathological mechanism of SCA7 does not involve a direct loss of SUMOylation after polyQ expansion of ATXN7.

How the SUMO modification of expanded polyQ ATXN7 influences its aggregation needs to be clarified in the future. SUMOylation could change interactions of ATXN7 with chaperones, which are always present in aggregates of several neurodegenerative diseases, including SCA7 (43) and which could be required for proper refolding or degradation. However, our observations that Hsp70 colocalized preferentially with the non-homogenous inclusions do not support this hypothesis. Alternatively, the attachment of SUMO could influence the three dimensional structure of ATXN7, resulting in modified solubility or self-assembly properties. Support for this hypothesis can be found in studies with SBMA: modification of the protein with a SUMO variant unable to interact with binding partners still reduced the aggregation of polyQ expanded androgen receptor (25).

Our observation that SUMOylation plays an important role in SCA7 by modifying the aggregation of the polyQ expanded ATXN7 suggests that cellular mechanisms modulating the SUMOylation pathway could be involved in SCA7 pathogenesis. Examples would be cell type-specific expression patterns of SUMO enzymes, other post-translational modifications, which interfere with SUMOylation (44) or oxidative stress, which has already been linked to neurodegenerative diseases (45) and also described to reversibly inhibit the SUMOylation pathway (46).

Our study demonstrates that SUMOylation, the first described post-translational modification of ATXN7, influences aggregation of polyQ expanded ATXN7, which is a key event during pathogenesis. Furthermore, our findings add the SUMOylation cascade, including modifying and demodifying enzymes, to the list of potential therapeutic targets to counteract disease progression.

MATERIALS AND METHODS

SCA7 patients: case histories and neuropathological findings

The detailed clinical histories and neuropathological findings in the SCA7 patients have been reported previously (6,8). Briefly, patient 1 was a 10-year-old boy who died 5 years after disease onset. At the age of 5 years, he had learning problems and progressive visual loss, and gradually developed cerebellar ataxia, clumsiness of the upper limb, dysarthria, and pigmentary degeneration. SCA7 was diagnosed by the presence of an 85 CAG repeat expansion in the SCA7 gene. He died of pneumopathy after several days in a coma. Neuropathological examination showed severe neuronal loss associated with gliosis in the inferior olive and cerebellar Purkinje cell layer. Neuronal inclusions were frequently found in inferior olive, lateral geniculate body, substantia nigra, and cerebral cortex. Patient 2 was a 36-year-old woman, whose initial symptoms, loss of visual acuity and gait disturbance, was noticed at age 22–23. She developed cerebellar dysarthria, truncal and limb ataxia, and dystonia in the upper extremities. The symptoms progressed gradually; at the age of 35 years, she was blind and wheelchair-bound. Molecular analysis showed that the patient carried a 49 CAG repeat expansion in the SCA7 gene. She died at the age of 36 years of an intercurrent disease. Neuropathologically, moderate to severe neuronal loss and gliosis were seen in the dentate nucleus, the inferior olive and Purkinje cell layer. Neuronal inclusions were frequently found in pontine nuclei, substantia nigra, red nucleus and cerebral cortex.

Plasmids and site-directed mutagenesis

The normal SCA7 construct, ATXN7-10Q, contains the full-length wild-type ATXN7 cDNA amplified by PCR from a previously described construct (7), inserted into *Eco*RI/*Xho*I site in the pCS2-HA vector. The pathological SCA7 construct ATXN7-72Q was made replacing the 10 repeat CAG sequence in ATXN7-10Q-pCS2 with a 72 CAG repeat sequence amplified by PCR from a previously described construct (7). The construct coding for PML IV in the pcDNA3 vector has already been described (21). FLAG-SUMO2-pSG5 and T7-PIASy-pSG5 were kind gifts from J. Seeler (Institut Pasteur, Paris). SUMO1 was cloned in frame with an N-terminal FLAG tag into vector pSG5. PIAS1, 3, xα and xβ were cloned in frame with N-terminal T7 tag into pSG5. The plasmids expressing Ubc9 and His-tagged SUMO1 and two have already been described (47). Construction coding for GCN5 in fusion with an N-terminus FLAG tag has been already described (4). ATXN7L3 and USP22 were cloned in fusion with an N-terminus FLAG tag in the pcDNA3 vector (5). The constructs ATXN7-10Q-K257R-pCS2 and ATXN7-10Q-K858R-pCS2 were obtained by site-directed mutagenesis with the QuickChange II Kit (Stratagene). ATXN7-72Q-K257R-pCS2 was obtained by fragment exchange from the ATXN7-10Q-K257R-pCS2 construct. All primer sequences used are available on request.

Cell culture, transfections

COS-7 and HeLa cells were maintained in DMEM (Invitrogen) supplemented with 10% fetal bovine serum and penicillin–streptomycin (100 UI/ml; 100 μg/ml). Cell lines were transfected with Lipofectamine-PLUS reagents (Invitrogen) as prescribed. HeLa cells were harvested directly in SDS sample buffer, after 36–48 h, for analysis by western blot. COS-7 cells were harvested, after 40–48 h, in the buffer mentioned below or analyzed by immunofluorescence 40–45 h post-transfection.

Western blot and filter retardation assay

Cells were rinsed twice with PBS and lysed 20 min on ice with buffer containing 50 mM Tris pH 8.0, 300 mM NaCl, 1% NP40, 1 mM EDTA, 20 mM NEM (Sigma) and 250 UI/ml benzonase (Merck) supplemented with a cocktail of protease inhibitors (Complete and Pefabloc, Roche). Protein concentrations of the total extracts were determined by Bio-Rad assay. Samples were prepared for western blot and for filter assay as previously described (48,49). For the filter assay, the

whole cell lysates were used and filtered through an acetate cellulose membrane (Schleicher and Schuell). Samples were analyzed by western blot on 4–12% polyacrylamide gels (Invitrogen).

Immunofluorescence, immunohistochemistry

COS-7 cells plated on glass coverslips coated with poly-lysine (Sigma) were fixed for 20 min with 4% paraformaldehyde. Permeabilization and incubations with antibodies were as previously described (48). Cells were mounted with Fluoromount-G and samples were observed with a Leica SP1 confocal microscope equipped with a 63×/1.32 numerical aperture (NA) objective. Leica confocal software was used to acquire images.

Mice were anaesthetized with pentobarbital (Sigma) and perfused transcardially with 4% paraformaldehyde in 0.1 M PBS, pH 7.4. Brains were removed and post-fixed for one night in the same solution. Brains were dehydrated, embedded in paraffin (Shandon Excelsior tissue processor from Thermo Scientific) and cut on a microtome into 5 μm-thick sections collected on slides. For immunohistochemistry, sections were deparaffinized in xylene and hydrated in a descending series of ethanol concentrations. Antigens were retrieved by boiling the sections in 0.01 M citrate buffer, pH 6.0, five times for 3 min in a microwave at 350 W. Sections were permeabilized and non-specific epitopes were blocked by incubation for 1 h in PBS containing: 3% BSA, 3% NGS, 0.1% Triton X-100. Sections were hybridized for 48 h at 4°C with a mix of the primary antibodies and the signal revealed by incubation with secondary antibodies for 2 h at room temperature.

Sections (6 μm) of formalin-fixed, paraffin-embedded cerebral cortex of the two patients (temporal cortex from Patient 1, and frontal cortex from Patient 2) were used for immunohistochemical staining. After pre-treatment, the sections were incubated with one of the primary antibodies and stained by 2,3-diaminobenzidine (DAB) hydrochloride as the chromogen (23). Double immunolabeling on the brain sections was performed with fluorescence labeled antibodies described in what follows.

Antibodies

For western blot (WB), filter assay (FA), immunofluorescence (IF) and immunohistochemistry (IHC) analysis, we used the following antibodies and concentrations: 1C1 mouse anti-ATXN7 (50) at 1:5000 (FA); mouse anti-HA (Babco) at 1:10000 (WB) and 1:4000 (IF); rabbit anti-ATXN7 (Affinity BioReagents) at 1:1000 (WB and IHC in knock-in mice); rabbit anti-ATXN7 (1261) (50*)* at 1:200 (IHC in human brain); rabbit anti-PML (H-238, Santa Cruz) at 1:500 (IF); 1C2 anti-polyQ monoclonal antibody at 1:2000 (FA); mouse anti-FLAG M2 (Sigma) at 1:5000 (WB); rabbit anti-SUMO1 (Abgent, AP1221a) at 1:100 (IF); rabbit anti-SUMO2 (Abgent, AP1282a) at 1:100 (IF), mouse anti-SUMO1 (GMP-1) (Zymed) at 1:1000 (IHC in knock-in mice) and at 1:800 (IHC in human brain); rabbit anti-cleaved caspase-3 (Asp175) (Cellsignal, 9661) at 1:400 (IF); mouse anti-Hsp70 (Stressgen) at 1:2000 (IF); mouse anti-19S5a proteasome subunit (Rpn10) (Biomol) at 1:4000 (IF); mouse anti-ubiquitinylated proteins (clone FK2) (Biomol) at 1:4000 (IF); mouse anti-gamma-tubulin (Sigma) at 1:5000 (WB). A newly developed mouse anti-SUMO1 antibody (3G12), raised against recombinant human SUMO1 (amino acids 1–97) fused to GST was used for IHC in human brain. The clone 3G12 was selected by the sensitive and specific immunoreactivity on formalin fixed paraffin embedded brain tissues. Screening was performed using paraffin embedded brain tissues of neuronal intranuclear inclusion disease, known to have SUMO1 positive neuronal inclusions (23). Immunoabsorption control study was done and the immunoreactivity was clearly absorbed after preabsorption with the immunized recombinant SUMO1. For immunofluorescence, secondary antibodies were: Alexa 488-conjugated donkey anti-mouse or donkey anti-rabbit IgG (Invitrogen) used at 1:1000 and CY3-conjugated donkey anti-mouse or donkey anti-rabbit IgG (Jackson Immunoresearch) used at 1:1000. The mouse anti-SUMO1 antibody (3G12) was directly conjugated with Alexa555, using Alexa Fluor Succinimidyl Esters (Molecular probes), and used for double immunolabeling. For western blot and filter assay, secondary antibodies were peroxidase-conjugated donkey anti-mouse or donkey anti-rabbit IgG (Jackson Immunoresearch) used at 1:50 000.

Co-immunoprecipitation

Each partner of the TFTC complex GCN5, ATXN7L3 or USP22 was transfected in COS-7 cells (90 mm culture dishes) in combination with wild-type ATXN7-10Q or variant ATXN7-10Q-K257R. Cells were harvested 42–45 h post-transfection and lyzed on ice in the following buffer: 25 mM Tris pH 8.0, 150 mM KCl, 5 mM $MgCl_2$, 1 mM EDTA, 0.1% NP40, 20 mM NEM, 250 UI/ml benzonase and 5% glycerol, supplemented with a cocktail of protease inhibitors (Complete, Pefablock). Total extracts were centrifuged at 13 000 rpm for 10 min at 4°C. For immunoprecipitation, supernatants were incubated with protein G Dynabeads (Invitrogen) coupled with anti-FLAG M2 (Sigma) or anti-myc (Santa cruz) antibodies for 2 h at 4°C on a rotating wheel. The beads were then washed three times with lysis buffer, and the bound proteins were directly denatured by heating for 5 min at 95°C in 30 μl Laemmli buffer. Samples were analyzed by western blot on 4–12% polyacrylamide gels (Invitrogen).

In vitro SUMOylation assay, nickel- and GST pulldown

The *in vitro* SUMOylation assay was performed on ^{35}S-labeled *in vitro* translated ATXN7 as described previously (51) using recombinant E1 (180 nM), Ubc9 (620 nM) and His-SUMO (7 μM). *In vitro* transcription/translation was performed using the TNT-coupled reticulocyte lysate system (Promega). Nickel pulldown from lysed cells transfected with ATXN7-10Q-pCS2 and His-SUMO1-pSG5 was performed as described (47,52). GST pulldown was done as in (51).

Quantification and statistical analysis

For all quantifications, results are presented as means ± SEM. For immunofluorescence experiments, 300 cells were counted in four independent manipulations. For the filter retardation assay, we quantified the non-saturated signals of four independent manipulations using Quantity One 4.4 software (Biorad). For statistical analysis, we performed *t*-test with SigmaStat 3.5 software (Systat software) and a *P*-value of <0.05 was considered statistically significant.

SUPPLEMENTARY MATERIAL

Supplementary Material is available at *HMG* online.

ACKNOWLEDGEMENTS

The authors are grateful to J.C. Rousselle and P. Lenormand for performing mass spectrometry, the cellular imagery platform of Salpêtrière hospital (PICPS) for confocal microscopy, N. Takabayashi, K. Iwabuchi for technical assistance, J. Seeler and all members of the Dejean lab for sharing reagents and advices, D. Devys for kind gift of antibodies and plasmids, H. Zoghbi and J. Gatchel for the SCA7 mice specimens, G. Stevanin for fruitful discussions and M. Ruberg for critical reading of the manuscript.

Conflict of Interest statement. None declared.

FUNDING

This study was funded by EuroSCA European consortium (contract number: LSHM-CT-2004-503304/E04004DD), Verum Foundation and La Ligue contre le Cancer (Equipe Labellisée). We thank the patient's association "Connaitre les Syndromes Cerebelleux" for a fellowship to A.J. and a grant to A.S. A.J. was supported by the French Ministry of Research and the Academie Nationale de Médecine, A.W. by the Fondation Recherche Medicale. J.T.F. was supported by Grant-in-Aid for Young Scientist (A) from the Japanese Ministry of Education, Science and Culture.

REFERENCES

1. David, G., Abbas, N., Stevanin, G., Durr, A., Yvert, G., Cancel, G., Weber, C., Imbert, G., Saudou, F., Antoniou, E. *et al.* (1997) Cloning of the SCA7 gene reveals a highly unstable CAG repeat expansion. *Nat. Genet.*, **17**, 65–70.
2. Cancel, G., Duyckaerts, C., Holmberg, M., Zander, C., Yvert, G., Lebre, A.S., Ruberg, M., Faucheux, B., Agid, Y., Hirsch, E. *et al.* (2000) Distribution of ataxin-7 in normal human brain and retina. *Brain*, **123**, 2519–2530.
3. Katsuno, M., Banno, H., Suzuki, K., Takeuchi, Y., Kawashima, M., Tanaka, F., Adachi, H. and Sobue, G. (2008) Molecular genetics and biomarkers of polyglutamine diseases. *Curr. Mol. Med.*, **8**, 221–234.
4. Helmlinger, D., Hardy, S., Sasorith, S., Klein, F., Robert, F., Weber, C., Miguet, L., Potier, N., Van-Dorsselaer, A., Wurtz, J.M. *et al.* (2004) Ataxin-7 is a subunit of GCN5 histone acetyltransferase-containing complexes. *Hum. Mol. Genet.*, **13**, 1257–1265.
5. Zhao, Y., Lang, G., Ito, S., Bonnet, J., Metzger, E., Sawatsubashi, S., Suzuki, E., Le Guezennec, X., Stunnenberg, H.G., Krasnov, A. *et al.* (2008) A TFTC/STAGA module mediates histone H2A and H2B deubiquitination, coactivates nuclear receptors, and counteracts heterochromatin silencing. *Mol. Cell.*, **29**, 92–101.
6. Takahashi, J., Fujigasaki, H., Zander, C., El Hachimi, K.H., Stevanin, G., Durr, A., Lebre, A.S., Yvert, G., Trottier, Y., de The, H. *et al.* (2002) Two populations of neuronal intranuclear inclusions in SCA7 differ in size and promyelocytic leukaemia protein content. *Brain*, **125**, 1534–1543.
7. Zander, C., Takahashi, J., El Hachimi, K.H., Fujigasaki, H., Albanese, V., Lebre, A.S., Stevanin, G., Duyckaerts, C. and Brice, A. (2001) Similarities between spinocerebellar ataxia type 7 (SCA7) cell models and human brain: proteins recruited in inclusions and activation of caspase-3. *Hum. Mol. Genet.*, **10**, 2569–2579.
8. Holmberg, M., Duyckaerts, C., Durr, A., Cancel, G., Gourfinkel-An, I., Damier, P., Faucheux, B., Trottier, Y., Hirsch, E.C., Agid, Y. *et al.* (1998) Spinocerebellar ataxia type 7 (SCA7): a neurodegenerative disorder with neuronal intranuclear inclusions. *Hum. Mol. Genet.*, **7**, 913–918.
9. Takahashi, J., Fujigasaki, H., Iwabuchi, K., Bruni, A.C., Uchihara, T., El Hachimi, K.H., Stevanin, G., Durr, A., Lebre, A.S., Trottier, Y. *et al.* (2003) PML nuclear bodies and neuronal intranuclear inclusion in polyglutamine diseases. *Neurobiol. Dis.*, **13**, 230–237.
10. Pennuto, M., Palazzolo, I. and Poletti, A. (2009) Post-translational modifications of expanded polyglutamine proteins: impact on neurotoxicity. *Hum. Mol. Genet.*, **18**, R40–R47.
11. Dorval, V. and Fraser, P.E. (2007) SUMO on the road to neurodegeneration. *Biochim. Biophys. Acta*, **1773**, 694–706.
12. Lieberman, A.P. (2004) SUMO, a ubiquitin-like modifier implicated in neurodegeneration. *Exp. Neurol.*, **185**, 204–207.
13. Johnson, E.S. (2004) Protein modification by SUMO. *Annu. Rev. Biochem.*, **73**, 355–382.
14. Seeler, J.S. and Dejean, A. (2003) Nuclear and unclear functions of SUMO. *Nat. Rev. Mol. Cell. Biol.*, **4**, 690–699.
15. Geiss-Friedlander, R. and Melchior, F. (2007) Concepts in sumoylation: a decade on. *Nat. Rev. Mol. Cell. Biol.*, **8**, 947–956.
16. Kerscher, O. (2007) SUMO junction-what's your function? New insights through SUMO-interacting motifs. *EMBO Rep.*, **8**, 550–555.
17. Poukka, H., Karvonen, U., Janne, O.A. and Palvimo, J.J. (2000) Covalent modification of the androgen receptor by small ubiquitin-like modifier 1 (SUMO-1). *Proc. Natl Acad. Sci. USA*, **97**, 14145–14150.
18. Riley, B.E., Zoghbi, H.Y. and Orr, H.T. (2005) SUMOylation of the polyglutamine repeat protein, ataxin-1, is dependent on a functional nuclear localization signal. *J. Biol. Chem.*, **280**, 21942–21948.
19. Steffan, J.S., Agrawal, N., Pallos, J., Rockabrand, E., Trotman, L.C., Slepko, N., Illes, K., Lukacsovich, T., Zhu, Y.Z., Cattaneo, E. *et al.* (2004) SUMO modification of Huntingtin and Huntington's disease pathology. *Science*, **304**, 100–104.
20. Mencia, M. and de Lorenzo, V. (2004) Functional transplantation of the sumoylation machinery into Escherichia coli. *Protein Expr. Purif.*, **37**, 409–418.
21. Janer, A., Martin, E., Muriel, M.P., Latouche, M., Fujigasaki, H., Ruberg, M., Brice, A., Trottier, Y. and Sittler, A. (2006) PML clastosomes prevent nuclear accumulation of mutant ataxin-7 and other polyglutamine proteins. *J. Cell. Biol.*, **174**, 65–76.
22. Matunis, M.J., Coutavas, E. and Blobel, G. (1996) A novel ubiquitin-like modification modulates the partitioning of the Ran-GTPase-activating protein RanGAP1 between the cytosol and the nuclear pore complex. *J. Cell. Biol.*, **135**, 1457–1470.
23. Takahashi-Fujigasaki, J., Arai, K., Funata, N. and Fujigasaki, H. (2006) SUMOylation substrates in neuronal intranuclear inclusion disease. *Neuropathol. Appl. Neurobiol.*, **32**, 92–100.
24. Yoo, S.Y., Pennesi, M.E., Weeber, E.J., Xu, B., Atkinson, R., Chen, S., Armstrong, D.L., Wu, S.M., Sweatt, J.D. and Zoghbi, H.Y. (2003) SCA7 knockin mice model human SCA7 and reveal gradual accumulation of mutant ataxin-7 in neurons and abnormalities in short-term plasticity. *Neuron*, **37**, 383–401.
25. Mukherjee, S., Thomas, M., Dadgar, N., Lieberman, A.P. and Iniguez-Lluhl, J.A. (2009) SUMO modification of the androgen receptor attenuates polyglutamine-mediated aggregation. *J. Biol. Chem*, **284**, 21296–21306.
26. Terashima, T., Kawai, H., Fujitani, M., Maeda, K. and Yasuda, H. (2002) SUMO-1 co-localized with mutant atrophin-1 with expanded polyglutamines accelerates intranuclear aggregation and cell death. *Neuroreport*, **13**, 2359–2364.

27. Denison, C., Rudner, A.D., Gerber, S.A., Bakalarski, C.E., Moazed, D. and Gygi, S.P. (2005) A proteomic strategy for gaining insights into protein sumoylation in yeast. *Mol. Cell. Proteomics*, **4**, 246–254.
28. Wohlschlegel, J.A., Johnson, E.S., Reed, S.I. and Yates, J.R. III (2004) Global analysis of protein sumoylation in Saccharomyces cerevisiae. *J. Biol. Chem.*, **279**, 45662–45668.
29. Meulmeester, E., Kunze, M., Hsiao, H.H., Urlaub, H. and Melchior, F. (2008) Mechanism and consequences for paralog-specific sumoylation of ubiquitin-specific protease 25. *Mol. Cell.*, **30**, 610–619.
30. Sterner, D.E., Nathan, D., Reindle, A., Johnson, E.S. and Berger, S.L. (2006) Sumoylation of the yeast Gcn5 protein. *Biochemistry*, **45**, 1035–1042.
31. Joseph, J., Tan, S.H., Karpova, T.S., McNally, J.G. and Dasso, M. (2002) SUMO-1 targets RanGAP1 to kinetochores and mitotic spindles. *J. Cell. Biol.*, **156**, 595–602.
32. Mahajan, R., Delphin, C., Guan, T., Gerace, L. and Melchior, F. (1997) A small ubiquitin-related polypeptide involved in targeting RanGAP1 to nuclear pore complex protein RanBP2. *Cell*, **88**, 97–107.
33. Muller, S., Matunis, M.J. and Dejean, A. (1998) Conjugation with the ubiquitin-related modifier SUMO-1 regulates the partitioning of PML within the nucleus. *EMBO J.*, **17**, 61–70.
34. Hilgarth, R.S., Murphy, L.A., Skaggs, H.S., Wilkerson, D.C., Xing, H. and Sarge, K.D. (2004) Regulation and function of SUMO modification. *J. Biol. Chem.*, **279**, 53899–53902.
35. Ross, C.A. and Poirier, M.A. (2004) Protein aggregation and neurodegenerative disease. *Nat. Med.*, **10** (suppl.), S10–S17.
36. Ross, C.A. and Poirier, M.A. (2005) Opinion: What is the role of protein aggregation in neurodegeneration? *Nat. Rev. Mol. Cell. Biol.*, **6**, 891–898.
37. Michalik, A. and Van Broeckhoven, C. (2003) Pathogenesis of polyglutamine disorders: aggregation revisited. *Hum. Mol. Genet.*, **12** (Spec. no 2), R173–R186.
38. Truant, R., Atwal, R.S., Desmond, C., Munsie, L. and Tran, T. (2008) Huntington's disease: revisiting the aggregation hypothesis in polyglutamine neurodegenerative diseases. *FEBS J.*, **275**, 4252–4262.
39. Sarge, K.D. and Park-Sarge, O.K. (2009) Sumoylation and human disease pathogenesis. *Trends Biochem. Sci.*, **34**, 200–205.
40. Ueda, H., Goto, J., Hashida, H., Lin, X., Oyanagi, K., Kawano, H., Zoghbi, H.Y., Kanazawa, I. and Okazawa, H. (2002) Enhanced SUMOylation in polyglutamine diseases. *Biochem. Biophys. Res. Commun.*, **293**, 307–313.
41. Chan, H.Y., Warrick, J.M., Andriola, I., Merry, D. and Bonini, N.M. (2002) Genetic modulation of polyglutamine toxicity by protein conjugation pathways in *Drosophila*. *Hum. Mol. Genet.*, **11**, 2895–2904.
42. Subramaniam, S., Sixt, K.M., Barrow, R. and Snyder, S.H. (2009) Rhes, a striatal specific protein, mediates mutant-huntingtin cytotoxicity. *Science*, **324**, 1327–1330.
43. Wyttenbach, A. (2004) Role of heat shock proteins during polyglutamine neurodegeneration: mechanisms and hypothesis. *J. Mol. Neurosci.*, **23**, 69–96.
44. Bossis, G. and Melchior, F. (2006) SUMO: regulating the regulator. *Cell. Div.*, **1**, 13.
45. Fatokun, A.A., Stone, T.W. and Smith, R.A. (2008) Oxidative stress in neurodegeneration and available means of protection. *Front. Biosci.*, **13**, 3288–3311.
46. Bossis, G. and Melchior, F. (2006) Regulation of SUMOylation by reversible oxidation of SUMO conjugating enzymes. *Mol. Cell.*, **21**, 349–357.
47. Seeler, J.S., Marchio, A., Losson, R., Desterro, J.M., Hay, R.T., Chambon, P. and Dejean, A. (2001) Common properties of nuclear body protein SP100 and TIF1α chromatin factor: role of SUMO modification. *Mol. Cell. Biol.*, **21**, 3314–3324.
48. Sittler, A., Walter, S., Wedemeyer, N., Hasenbank, R., Scherzinger, E., Eickhoff, H., Bates, G.P., Lehrach, H. and Wanker, E.E. (1998) SH3GL3 associates with the Huntingtin exon 1 protein and promotes the formation of polygln-containing protein aggregates. *Mol. Cell.*, **2**, 427–436.
49. Wanker, E.E., Scherzinger, E., Heiser, V., Sittler, A., Eickhoff, H. and Lehrach, H. (1999) Membrane filter assay for detection of amyloid-like polyglutamine-containing protein aggregates. *Methods Enzymol.*, **309**, 375–386.
50. Yvert, G., Lindenberg, K.S., Picaud, S., Landwehrmeyer, G.B., Sahel, J.A. and Mandel, J.L. (2000) Expanded polyglutamines induce neurodegeneration and trans-neuronal alterations in cerebellum and retina of SCA7 transgenic mice. *Hum. Mol. Genet.*, **9**, 2491–2506.
51. Bischof, O., Schwamborn, K., Martin, N., Werner, A., Sustmann, C., Grosschedl, R. and Dejean, A. (2006) The E3 SUMO ligase PIASy is a regulator of cellular senescence and apoptosis. *Mol. Cell.*, **22**, 783–794.
52. Muller, S., Berger, M., Lehembre, F., Seeler, J.S., Haupt, Y. and Dejean, A. (2000) c-Jun and p53 activity is modulated by SUMO-1 modification. *J. Biol. Chem.*, **275**, 13321–13329.